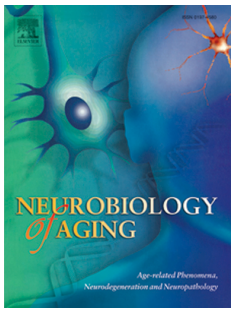

Disruption of oligodendrocyte progenitor cells is an early sign of pathology in the triple transgenic mouse model of Alzheimer's disease

Ilaria Vanzulli, Maria Papanikolaou, Irene Chacon De La Rocha, Francesca Pieropan, Andrea D. Rivera, Diego Gomez-Nicola, Alexei Verkhratsky, José Julio Rodríguez, Arthur M. Butt

PII: S0197-4580(20)30185-8

DOI: https://doi.org/10.1016/j.neurobiolaging.2020.05.016

Reference: NBA 10859

To appear in: *Neurobiology of Aging*

Received Date: 15 April 2020

Revised Date: 29 May 2020

Accepted Date: 31 May 2020

Please cite this article as: Vanzulli, I., Papanikolaou, M., De La Rocha, I.C., Pieropan, F., Rivera, A.D., Gomez-Nicola, D., Verkhratsky, A., Rodríguez, J.J., Butt, A.M., Disruption of oligodendrocyte progenitor cells is an early sign of pathology in the triple transgenic mouse model of Alzheimer's disease, *Neurobiology of Aging* (2020), doi: https://doi.org/10.1016/j.neurobiolaging.2020.05.016.

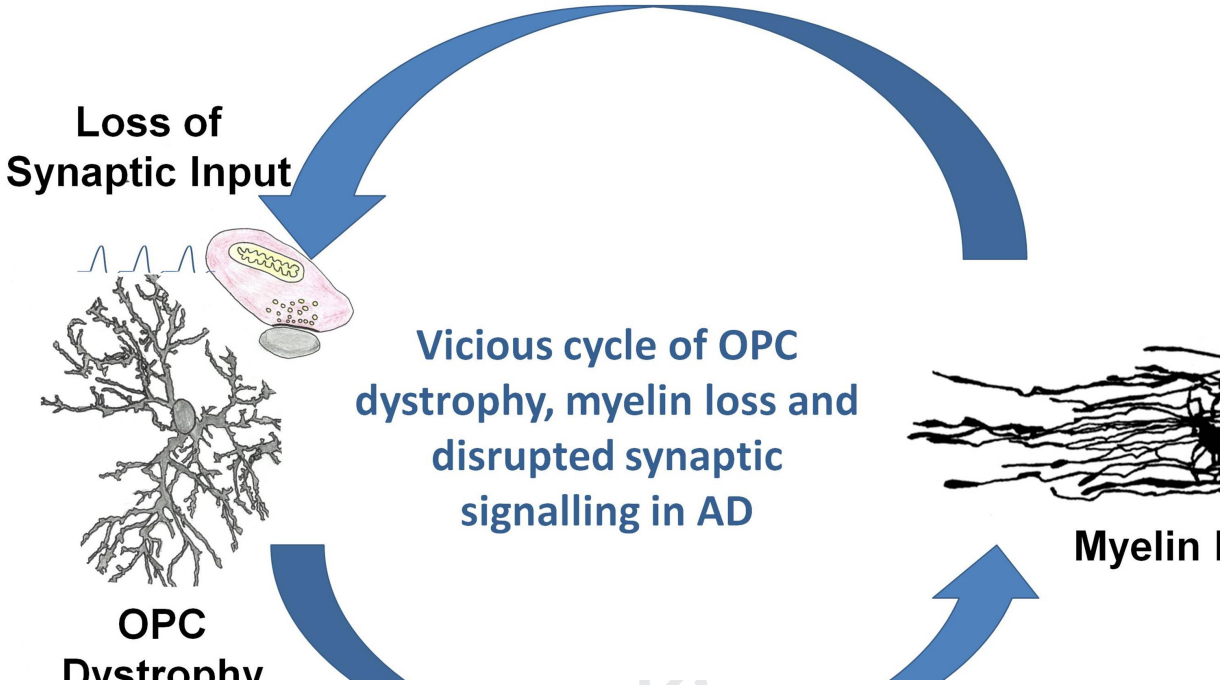
Loss of
Synaptic Input
Vicious cycle of OPC dystrophy, myelin loss and disrupted synaptic signalling in AD
OPC
Dystrophy
Myelin

Neurobiology of Ageing

Disruption of oligodendrocyte progenitor cells is an early sign of pathology in the triple transgenic mouse model of Alzheimer's disease

Ilaria Vanzulli[1], Maria Papanikolaou[1], Irene Chacon De La Rocha[1], Francesca Pieropan[1], Andrea D. Rivera[1], Diego Gomez-Nicola[7], Alexei Verkhratsky[5,6], José Julio Rodríguez[2,3,42,3] and Arthur M. Butt[1*]

[1]*Institute of Biomedical and Biomolecular Sciences, School of Pharmacy and Biomedical Sciences, University of Portsmouth, UK.*

[2]*BioCruces Health Research Institute, 48903, Barakaldo, Spain*

[3]*Department of Neuroscience, University of the Basque Country UPV/EHU, 48940, Leioa, Spain*

[4]*IKERBASQUE, Basque Foundation for Science, 48013-Bilbao, Medical School, Spain*

[5]*Faculty of Biology, Medicine and Health, University of Manchester, UK.*

[6]*Achúcarro Basque Center for Neuroscience, IKERBASQUE, Basque Foundation for Science, 48011, Bilbao, Spain.*

[7]*School of Biological Sciences, University of Southampton, Southampton, SO17 1BJ, UK.*

*Corresponding author: Arthur M. Butt, Email: arthur.butt@port.ac.uk

Abstract

There is increasing evidence that myelin disruption is related to cognitive decline in Alzheimer´s disease (AD). In the CNS, myelin is produced by oligodendrocytes, which are generated throughout life by adult oligodendrocyte progenitor cells (OPCs), also known as NG2-glia. To address whether alterations in myelination are related to age-dependent changes in OPCs, we analysed NG2 and myelin basic protein (MBP) immunolabelling in the hippocampus of 3×Tg-AD mice at 6 and 24 months of age, compared with non-Tg age-matched controls. There was an age-related decrease in MBP immunostaining and OPC density, together with a decline in the number of OPC sister cells, a measure of OPC replication. Notably, the loss of myelin and OPC sister cells occurred earlier at 6 months in 3xTg-AD, suggesting accelerated ageing, although there was not a concomitant decline in OPC numbers, suggesting the observed changes in myelin were not a consequence of replicative exhaustion, but possibly of OPC disruption or senescence. In line with this, a key finding is that compared to age-match controls, OPC displayed marked morphological atrophy at 6 months in 3xTg-AD followed by morphological hypertrophy at 24 months, as deduced from significant changes in total cell surface area, total cell volume, somata volume and branching of main processes. Moreover, we show that hypertrophic OPCs surround and infiltrate amyloid-β (Aβ) plaques, a key pathological hallmark of AD. The results indicate that OPCs undergo complex age-related remodelling in the hippocampus of the 3xTg-AD mouse model. We conclude that OPC disruption is an early pathological sign in AD and is a potential factor in accelerated myelin loss and cognitive decline.

Key Words: oligodendrocyte progenitor cell, OPC, glia, hippocampus, astrocyte, amyloid β, Alzheimer's disease

1. Introduction

Alzheimer's disease (AD) is a neurodegenerative disease characterised by age-related decline in learning, memory and cognition. Neuropathological hallmarks of AD are amyloid β (Aβ) plaques and neurofibrillary tangles (NFTs). In addition, myelin disruption is prominent in AD (Bartzokis 2011a), while myelin loss may predict AD onset and neurodegenerative changes in humans (Brickman et al 2015), as well as in animal models of AD (Desai et al 2009). Thus, disruption of myelination is a feature of AD, although the underlying causes are unresolved.

In the CNS, myelin is produced by oligodendrocytes, which are generated from oligodendrocyte progenitor cells (OPCs) (Rivers et al 2008, Zhu et al 2011), also known as NG2-glia or synantocytes (Butt et al 2005). OPCs are identified by their expression of the membrane proteoglycan NG2 (Cspg4) (Stallcup 1981), and are the main proliferative cells in the brain (Dawson et al 2003). In the adult brain, OPCs slowly divide asymmetrically to form daughter cells that are responsible for OPC self-renewal and for generating new oligodendrocytes for myelin repair and for myelination of new connections important in learning (Hughes et al 2018, McKenzie et al 2014, Xiao et al 2016, Young et al 2013). In addition, OPCs readily respond to CNS pathology by a characteristic morphological remodeling and increased NG2 expression (Levine 2016, Rodríguez et al 2016). Notably, OPCs display increased senescence and disruption in the aging brain (Neumann et al 2019, Segel et al 2019, Sim et al 2002), and this may be aggravated in human and mouse AD (Dong et al 2018, Li et al 2013, Nielsen et al 2013, Zhang et al 2019b). These studies suggest that age-related changes in OPCs are related to a reduction in myelination in AD (Butt et al 2019).

The triple transgenic mouse model of AD (3xTg-AD) harbours presenilin 1 (PS1; M146V), amyloid precursor protein (APP; Swe), and tau (P301L) transgenes, and displays progressive AD-like pathology and cognitive impairments in an age-related manner (Belfiore et al 2019, Oddo et al 2003, Olabarria et al 2010). Immunohistochemical, electron microscope and imaging studies have shown myelin disruption in the hippocampus of 3×Tg-AD mice in 6 month-old mice (Desai et al 2010, Desai et al 2009, Nie et al 2019), concomitant with the appearance of Aβ plaques (Oddo et al 2003). Here, we have performed a detailed

examination of age-related changes in OPC in the hippocampus of 3xTg-AD mouse. Morphological analysis (Olabarria et al 2010) of total cell surface area, total cell volume, somata volume and branching of main processes demonstrated that OPC display a marked morphological atrophy at 6 months in 3xTg-AD. Morphological atrophy was collateral to a decline in the numerical density of OPC daughter cells and decreased myelin immunostaining in the hippocampus. In contrast, at 24 months in 3xTg-AD OPCs undergo a marked morphological hypertrophy and cluster around Aβ plaques with astrocytes. This study identifies complex changes in OPC morphology that are related to the pathogenesis of AD.

2. Materials and methods

2.1. Animals and tissues

All animal procedures were carried out in accordance with the United Kingdom Animals (Scientific Procedures) Act of 1986 under licence from the Home Office. All efforts were made to reduce the number of animals by following the 3Rs. The procedure for generating 3xTg-AD mice has been described previously (Oddo et al., 2003; Rodríguez et al., 2008). The 3xTg-AD mouse line harbours the APP Swedish mutations K670N/M671L, the presenilin-1 M146V mutation and the tau P301L mutation in a C57BL6 mice background, and all 3xTg-AD and non-Tg control mice were obtained by crossing homozygous breeders. The animals were housed in same-sex cages, kept in 12 h light-dark cycles with free access to food and water independent of the diet. at these ages that the amyloid and tau pathologies emerge resembling the human Alzheimer's disease progression. Mice aged 6 and 24 months were used, because 3xTg-AD mice have been shown to exhibit myelin disruption at 6 months prior to deposition of extracellular Aβ plaques, which are prominent at 24 months of age (Desai et al 2010, Olabarria et al 2010). Male 3xTgAD and non-transgenic control mice were anaesthetized with intra-peritoneal injection of sodium pentobarbital (50 mg kg) at 6 and 24 months of age. The mice were perfused through the aortic arch with 3.75% acrolein (TAAB, Berkshire, UK) in a solution of 2% paraformaldehyde (Sigma, Cambridge, UK) and 0.1 M phosphate buffer (PB) pH 7.4, followed by 2% paraformaldehyde.

2.2 Immunohistochemistry

Brains were removed and cut into 4- to 5-mm coronal slabs of tissue containing the entire rostrocaudal extent of the hippocampus. Brain sections were postfixed in 2% paraformaldehyde for 24 h and kept in 0.1 M PB, pH 7.4. Coronal sections of the brain were cut into 40 μm thickness using a vibrating microtome (VT1000S; Leica, Milton Keynes, UK). Free floating brain sections in 0.1 M PB, pH 7.4, were collected and stored in cryoprotectant solution containing 25% sucrose and 3.5% glycerol in 0.05 M PB at pH 7.4. Coronal sections at levels -1.58 ⁄ -2.46 mm (hippocampus) posterior to bregma were selected for immunohistochemistry according to the mouse brain atlas. The sections were incubated for 30 min in 30% methanol in 0.1 M PB and 3% hydrogen peroxide (H_2O_2) (Sigma). Sections were then rinsed with 0.1 M PB for 5 min and placed in 1% sodium borohydride (Sigma) for 30 min. The sections were then washed with PB profusely before rinsing in 0.1 M Trizma

base saline (TS) for 10 min. Brain sections were then incubated in 0.5% bovine serum albumin (BSA) (Sigma) in 0.1 M TS and 0.25% Triton (Sigma) for 30 min. Sections were incubated for 24 h at room temperature in primary antibody: rabbit anti-NG2, 1:400 (Millipore); rat anti-MBP, 1:400 (Millipore); mouse anti-Aβ , 1:1000 (Covance). Tissues were then washed 3 times again in TS and incubated with the appropriate secondary antibody (AlexaFluor® 488, AlexaFluor® 568, 1:400, Life Technologies) diluted in blocking solution for 1 hr at room temperature on an orbital shaker and protected from the light. Following secondary antibody incubation, tissues were washed 2 times with TS and 3 times with PB before being covered with mounting medium and glass coverslips ready for imaging.

2.3 Confocal Microscopy and Image Analysis

Images were captured using a Zeiss Axiovert LSM 710 VIS40S confocal microscope and maintaining the acquisition parameters constant to allow comparison between samples within the same experiment. Acquisition of images was done with x20 objective for cell counts and analysis of MBP immunostaining; x40 objective was used to examine relationships between OPCs and Aβ plaques; x100 objective was used for OPC 3D reconstruction and morphological analysis, with *z*-stacks formed by 80-100 single plains with an interval of 0.3 µm.

2.4 Quantification

Cell counts for OPCs were performed in a constant field of view (FOV) of 100 µm x100 µm in projected images of z-stacks of 10 optic sections with 1µm interval. Morphological analyses of NG2-glia was performed as previously used for astrocytes in the 3xTg-AD mouse (Olabarria et al 2010), using the *Cell Analyst* programme and morphological calculations detailed in Chvatal et al. (2007). In brief, the *Cell Analyst* programme builds a detailed 3-D reconstruction of the cell based on a series of high resolution confocal z-stacks 0.2 µm apart, which defines the precision of the analysis (Chvátal et al 2007); we used five digital filters (average 3×3, convolution, gauss 5×5, despeckle, simple objects removal) and a threshold of 50 to determine the surface and volume of the NG2-positive OPCs (Olabarria et al 2010). Relative density of MBP immunostaining was measured from a constant field of view using ImageJ; a threshold was set from negative controls and parameters were kept constant to avoid experimental errors and/or bias. Results are expressed as mean ± SEM

and statistical differences were determined by one-way ANOVA and Newman–Keuls multiple comparison *post-hoc* analysis or unpaired t-tests, as appropriate, using Graphpad Prism5.0.

3. Results

3.1. Age-related changes in OPC numbers and MBP immunolabelling

Disruption of oligodendrocytes and myelin is an early event in the hippocampus of 3xTg-AD mice (Desai et al 2010, Desai et al 2009), but it is unclear how this is related to age-related changes in OPCs, which are responsible for life-long generation of myelinating oligodendrocytes (Young et al 2013). To examine this, we performed immunostaining for NG2 and MBP in 6 and 24 month old 3xTg-AD, compared to age-matched controls (Fig. 1). NG2-positive OPCs were widely distributed throughout the hippocampus of both 3xTg-AD and non-Tg mice (Fig. 1A1-iv), and cell counts indicated there was a decrease in the overall numerical density of OPCs between 6 months and 24 months in both 3xTg-Ad and non-Tg controls (Fig. 1Av, unpaired t-tests). In addition, we observed an age-related decrease in MBP immunostaining between 6 months and 24 months in non-Tg controls (Fig 1Bi, iii), however this decrease occurred earlier in 3xTg-AD at 6 months (Fig. 1Biii), without further change at 24 months (Fig. 1Biv). Quantitative analysis confirmed that MBP immunofluorescence intensity was significantly less in 6-month 3xTg-AD hippocampus compared to age-matched non-Tg controls (Fig. 4E; $p<0.001$) and equivalent to the level seen in 24-month controls. The results demonstrate a decline in OPCs and MBP with physiological ageing, but although OPC numerical density was unaltered in 3xTg-AD, the loss of MBP was significantly accelerated.

3.2. Age-related changes in OPC sister cells

Similarly to stem cells, OPCs self-maintain by undergoing asymmetric division and recently divided cells occur as closely associated duplets or triplets of 'daughter cells' that either self-sustain OPCs or proceed to differentiate into oligodendrocytes (Boda et al 2014). Hence, the frequency of OPC duplets/triplets is a measure of cell division and OPC regenerative potential (Boda et al 2014). To examine this in ageing, NG2 immunostaining was performed together with nuclear labelling with Hoechst blue to highlight groups of two or more juxtaposed OPC daughter cells (Fig. 2). OPC doublets and triplets were prominent throughout the hippocampus in 6 month non-Tg controls, exemplified in the CA1 (Fig. 2A). Quantitation shows a significant decrease in OPC daughter cells between 6 and 24 months in non-Tg controls in the hippocampus overall (Fig. 2B; $p<0.001$, ANOVA with Newman–Keuls multiple comparison *post-hoc* analysis), and regional analyses demonstrated

equivalent decline in the dentate gyrus (DG), and CA1 and CA3 regions (Fig. 2C-E). At 6 months, the number of OPC daughter cells was significantly less in 3xTg-AD hippocampus than age-matched controls (Fig. 2B; $p<0.001$), and declined to the level seen at 24-months in controls (Fig. 2B-E). There was no further change in OPC daughter cells at 24 months in 3xTg-AD, which was equivalent to age-matched controls (Fig. 2B-E). The results support a decline in OPC replication in physiological ageing that is observed at a younger age in 3xTg-AD.

3.3. Age-related changes in OPC morphology

Changes in the cellular morphology of OPCs is a characteristic of the response to CNS pathology (Levine 2016, Rodríguez et al 2016) and has been reported in human AD and mouse models of the disease (Dong et al 2018, Li et al 2013, Nielsen et al 2013, Zhang et al 2019b). To examine whether this occurs in 3xTg-AD, we performed a detailed morphological analysis of NG2 immunostained OPCs in the hippocampus at 6 and 24 months (Fig. 3), using the *Cell Analyst* programme and morphological parameters detailed by Chvatal et al. (2007), as described previously for in astrocytes in the 3xTg-AD model (Rodríguez et al 2013). The results show no significant difference in the morphology of OPCs at 6 and 24 months in non-Tg controls (Fig. 3A, C), also confirmed by quantification of multiple cellular morphological parameters (Fig. 3E-H). In contrast, at 6 months OPCs displayed marked morphological atrophy in 3xTg-AD, compared to controls (Fig. 3A, B), exhibiting a significant decrease in overall cell size and size of cell somata (Fig. 3E-H). Conversely, at 24 months OPCs displayed marked hypertrophy in 3xTg-AD, compared to age-matched controls (Fig. 3C, D), and 6 month 3xTg-AD (Fig. 3B), with significantly larger cell volume and surface area (Fig. 3E, H) and of cell somata volume and surface area (Fig. 3F, G). It is notable that NG2-glia have circular domains in the x-y plane, but are extremely flat in the z-plane, and their somata are not spherical, but instead appear as a 'fjord-like' in the x-y planes, and extremely thin in the z-plane (Fig. 2Aii, Aiii), hence surface-volume relationships are not simple cubic as for a sphere. Overall, the surface-volume ratio is $\geq$ 10 in NG2-glia, as it is in astrocytes, although NG2-glia are much smaller and the overall values are correspondingly 2-3 times smaller than equivalent measurements in astrocytes (Chvátal et al 2007, Olabarria et al 2010). The results demonstrate OPCs go through complex morphological changes in 3xTg-AD that are not

observed in natural ageing, characterised by shrinkage in early AD, followed by a clear hypertrophy at late stages, indicative of a reactive metamorphosis.

3.4. OPCs are closely localised with Aβ plaques in 3xTg-AD

Neuropathological changes and Aβ plaque load become significantly greater with age in 3xTg-AD mice in AD-relevant brain regions, including the hippocampus (Belfiore et al 2019, Oddo et al 2003). There is evidence from *in vitro* studies that Aβ is toxic for OPCs (Desai et al 2011) and induces morphological condensation (Nielsen et al 2013). However, we did not observe a decrease in OPC in 3xTg-AD and cells were hypertrophic at 24 months. We therefore performed double immunfluorescence labelling to examine the relations between OPCs and Aβ plaques in 24 month 3xTg-AD (Fig. 4). The results demonstrate that hypertrophic OPCs are adjacent to Aβ plaques throughout the hippocampus (Fig. 4A). Higher magnification imaging in the CA1 hippocampal area demonstrates the intimate relationships between OPCs and Aβ plaques (Fig. 4B-D). Large Aβ plaques are circumscribed by OPCs and infiltrated by their processes (Fig. 4B). OPCs were observed to be located both between multiple plaques that they contact (Fig. 4C), as well as being embedded within Aβ plaques (Fig. 4D). In the cortex, intraneuronal and vascular Aβ immunoreactivity was prominent in 24 month 3xTg-AD (Fig. 5A, C), and OPCs were directly apposed to these, surrounding them with their processes (Fig. 5B, D). The results demonstrate that OPCs are intimately associated with Aβ plaques in 3xTg-AD, consistent with a recent study in human AD (Zhang et al 2019b).

3.5. Interrelations between OPCs and astrocytes in Aβ plaques

In 3xTg-AD, astrocyte hypertrophy is associated with Aβ plaques (Olabarria et al 2010), and there is evidence astrocytes play a role in the clearance and removal of Aβ (Nielsen et al 2010). The close associations of OPC with Aβ plaques demonstrated above stimulated us to examine their interrelationships with astrocytes in the 24-month 3xTg-AD hippocampus (Fig. 6). Triple immunostaining for NG2, GFAP and Aβ shows that both astrocytes and OPCs are densely distributed throughout the hippocampus in association with Aβ deposits (Fig. 6A), and the processes of OPCs and astrocytes overlap extensively, contacting and infiltrating proximal Aβ plaques (Fig. 6B). Furthermore, in the hippocampus of 24 month 3xTg-AD we

occasionally observed cells co-immunostained for NG2 and GFAP (Fig. 6C, D). NG2 positive astrocytes have been reported in human AD in individuals with high Aβ plaque load (Nielsen et al 2013), and comparison with NG2+/GFAP- OPCs and NG2-/GFAP+ astrocytes in the same field of view in our study indicates NG2+/GFAP+ cells had a morphology more akin to astrocytes than OPCs (Fig. 6D). Our results demonstrate that OPCs and astrocytes cluster around the same Aβ plaques in 3xTg-AD.

4. Discussion

Age-related loss of myelin is a feature of normal aging and has been shown to be exacerbated in human AD (Bartzokis 2011a, Brickman et al 2015) and in multiple animal models of AD-like pathology (Desai et al 2009, Dong et al 2018). Here, we confirm previous observations (Desai et al 2010, Desai et al 2009), by showing that compromised myelination is evident at 6 months of age in 3xTg-AD, to a degree comparable to that observed at 24 months in natural aging. The maintenance of myelination in the adult brain is an ultimate function of OPCs, which divide and regenerate oligodendrocytes more slowly in the ageing brain (Psachoulia et al 2009, Young et al 2013). Our data shows an age-related decrease in the number of OPC daughter cells occurred significantly earlier, at 6 months, in 3xTg-AD, suggesting OPC self-renewal is compromised at early stages of AD-like pathology. Notably, OPCs displayed marked cellular shrinkage at 6 months in 3xTg-AD. In contrast, OPCs were hypertrophic at 24 months in 3xTg-AD and, together with astrocytes, were closely associated with Aβ plaques (Li et al 2013, Nielsen et al 2010). Our findings indicate complex changes in OPCs are important markers for early and late stages of AD-like pathology, which may be a major factor in myelin loss.

Imaging studies in 3xTg-AD show pronounced myelin changes in the fimbria, which acts as the major output tract of the hippocampus (Nie et al 2019), and our results support evidence that myelination is reduced in 3xTg-AD (Desai et al 2011, Desai et al 2010, Desai et al 2009, Mastrangelo & Bowers 2008). These results in 3xTg-AD mice correlate well with imaging and postmortem studies in human AD demonstrating widespread abnormalities in oligodendrocytes and myelin, including reduced MBP (Bartzokis 2011b, De Rossi et al 2016, Ihara et al 2010, McKenzie et al 2017, Nasrabady et al 2018, Roher et al 2002). Indeed, white matter changes are an early feature of human AD (Fischer et al 2015, Hoy et al 2017), and the premature loss of MBP immunostaining observed in our study is consistent with myelin loss being an early event in AD pathology and cognitive decline (Butt et al 2019, Nasrabady et al 2018, Wang et al 2020). Certainly, myelin disruption is coincident with the earliest signs of cognitive impairment and neuropathology in 3xTg-AD (Billings et al 2005, Oddo et al 2003). Furthermore, myelin disruption has been shown to result in axonal and neuronal degeneration (Stassart et al 2018), and myelin injury and loss of oligodendrocytes in AD is associated with axon degeneration and amyloid plaques (Mitew et al 2010, Zhan et al 2015).

The causes of myelin loss in AD are likely to include direct Aβ toxicity (Desai et al 2011), as well as glutamate, metabolic and iron dyshomeostasis (Ndayisaba et al 2019, Wang & Reddy 2017, Yin et al 2016). Our results indicate disruption of OPCs is another key event that may contribute to myelin loss in early AD.

At early stages of disease progression in 3xTg-AD, OPCs displayed a striking morphological atrophy, manifested by decreased cell surface area and volume, concomitant with a >30% decrease in OPC daughter cells, a measure of their recent cell division (Boda et al 2014). The asymmetric division of OPCs is critical for self-replication and the life-long generation of new myelinating oligodendrocytes as required (Dimou et al 2008, Kang et al 2010, Rivers et al 2008, Zhu et al 2008). Hence, the early atrophy of OPCs and apparent decrease in self-renewal indicates disruption of OPCs may be a key factor in the accelerated loss of myelin in 3xTg-AD. Notably, OPCs extend processes to contact glutamatergic synapses in the hippocampus (Bergles et al 2000), and glutamatergic signalling promotes OPC proliferation and differentiation (Chen et al 2018, Wake et al 2011). It is significant, therefore, that synaptic dysfunction, in particular disruption of glutamatergic signalling, is an early event in 3xTg-AD (Chakroborty et al 2019, Clark et al 2015, Oddo et al 2003), and is a major component of human AD (Crimins et al 2013). Astroglial glutamate homeostasis is also dysregulated in 3xTg-AD (Kulijewicz-Nawrot et al 2013, Olabarria et al 2010), which would further exacerbate glutamate signalling onto OPCs. The atrophy of OPC processes is contemporaneous with disruption of synaptic signalling, suggesting this is an important factor in the observed decline in OPC self-renewal and reduced capacity for replacing myelin lost in AD (Rivera et al 2016). Overall, OPC numbers did not decline until later ages in 3xTg-AD, implying the accelerated decline in myelination in 3xTg-AD was not directly related to a loss of OPCs, but may reflect reduced differentiation and OPC senescence (Zhang et al 2019a). At later stages of disease progression OPCs displayed a marked hypertrophy in 3xTg-AD, with increased cell volume and surface area, thicker processes and enlarged cell bodies, characteristic of an injury response in OPCs (Ong & Levine 1999). Hypertrophic OPCs contacted Aβ plaques together with astrocytes, which have been described previously (Rodríguez et al 2008). These findings are consistent OPCs being relatively resistant to Aβ

(Horiuchi et al 2012), and there is evidence OPCs are involved in Aβ clearance (Li et al 2013, Nielsen et al 2010).

In conclusion, the results demonstrate that OPCs undergo complex changes that are related to accelerated myelin loss in 3xTg-AD. This study highlights the importance of OPCs in AD pathogenesis.

Acknowledgements
Supported by grants from the BBSRC (AB, AR, Grant Number BB/M029379/1), MRC (AB, MP, Grant Number MR/P025811/1), Alzheimer's Research UK (DG, AB, Grant Number PG2014B-2), EU Marie Curie Framework 7 (AB, AV, IV), University of Portsmouth PhD Programme (AB, ICR), Spanish Ministerio de Economía y Competitividad, RETOS Colaboración (JJR, Grant Number RTC-2015-3542-1, co-financed by FEDER).

Disclosure Statement

AB and AR are shareholders in the company GliaGenesis. The authors declare no other conflicts.

Figure Legends

Figure 1 Age-dependent changes in OPCs and myelin in the hippocampus of 3xTg-AD and age-matched non-Tg controls. (**Ai-iv, B-iv**) Confocal images illustrating the hippocamous immunolabelled with the OPC marker NG2 (Ai-iv) and the myelin marker MBP (**Bi-iv**). Scale bars=50 μm. (Av, Bv) Bar graphs showing the numerical density of NG2+ OPCs (Av) and MBP immunoreactive intensity in the hippocampus; data are mean ± SEM, **p*<0.05, ***p*<0.01, unpaired t-tests.

Figure 2 Age-dependent changes in OPC daughter cells in hippocampus of 3xTg-AD and age-matched non-Tg controls. (A) Confocal images illustrating OPC duplets (arrows), in the CA1 area of the hippocampus of 3xTg-AD mice immunolabelled for NG2 (green) and counterstained with the nuclear marker Hoechst blue (blue). Maximum intensity *z*-stack projection (Ai), together with single z-section (Aii) and orthogonal section through the *x-x* plane (Aiii), showing juxtaposed duplets of recently divided OPC daughter cells. Scale bars = 20 μm in Ai and 10 μm in Aii, Aiii. **(B-E)** Quantification of sister cells per constant field of view (FOV) in the hippocampus overall (B), the dentate gyrus (DG) (C), CA1 (D) and CA3 (E); data are mean ± SEM from 3 sections per animal, *n*=3 animals. **p<0.05, **p<0.01, ***p<0.001,* unpaired t-tests.

Figure 3 Age-dependent changes in OPC morphology in the CA1 hippocampus of 3xTg-AD and age-matched non-Tg controls. (**A**-**D**) Representative confocal images of OPCs in the CA1 region of the hippocampus, illustrating in magenta the outline used for analysis of individual cells using the *Cell Analyst* programme (Chvátal *et al.*, 2007); scale bars=10 μm. (**E**-**H**) Quantification of OPC total cell volume (**E**), total cell surface area (**F**), cell body volume (**G**) and cell body surface area (**H**); data are mean ± SEM from 25 cells from 3 sections per mouse, where *n*=3 or 4). *p<0.05, **p<0.01, ****p<0.0001 unpaired t-tests.

Figure 4 Relationships between OPCs and Aβ plaques in the hippocampus of 24-month 3xTg-AD. Confocal images of coronal brain sections from 24-month 3xTg-AD double immunostained for NG2 (green) and Aβ (red). (A) Overview of the association of OPCs with Aβ in the CA1 layersof the hippocampus, with merged image (Ai) and indvidual channels for NG2 (Aii) and Ab(Aiii). (B) OPCs clustering around Aβ plaque in maximum intensity *z*-stack projection (Bi) and single z-section (Bii). (C) Maximum intensity *z*-stack projection of OPC within the boundary of multiple Aβ plaques. (D) OPC embedded within an Aβ plaque in maximum intensity *z*-stack projection (Fi) and orthogonal section (Fii). Scale bars = 50 μm in A , 25 mm in B and 20 μm in C, D.

Figure 5 Relationship of OPCs with intraneuronal and vascular Aβ in 3xTg-AD. Confocal images of 24 month 3xTg-AD cortex double immunostained for NG2 (green) and Aβ (red). OPCs are directly apposed to Aβ containing neurones (A, B) and blood vessels (C, D). Scale bars = 100 μm in A, C, and 20 μm in B, D.

Figure 6 Interrelations between OPCs and astrocytes with Aβ plaques in the 24-month 3xTg-AD hippocampus. Confocal images of CA1 region triple immunostained for NG2 (green), GFAP (red) and Aβ (blue). (**A**) OPCs and astrocytes are uniformly distributed in the CA1 layer with overlapping process domains. (**B**) OPCs and astrocytes are associated with the same Aβ plaques, with processes intertwined within Aβ plaques. (**C**) Large Aβ plaque containing cells co-expressing NG2 and GFAP (arrows, colocalization appears yellow). (**D**) High magnification maximum intensity *z*-stack projection of a NG2+/GFAP+ cell (asterisk), illustrating merged image (D), together with individual channels for NG2 (Di) and GFAP (Dii). Scale bars = 50 μm in A, 10 μm in B, D, and 30 μm in C.

References

Bartzokis G. 2011a. Alzheimer's disease as homeostatic responses to age-related myelin breakdown. *Neurobiology of aging* 32: 1341-71

Bartzokis G. 2011b. Alzheimer's disease as homeostatic responses to age-related myelin breakdown. *Neurobiol Aging* 32: 1341-71

Belfiore R, Rodin A, Ferreira E, Velazquez R, Branca C, et al. 2019. Temporal and regional progression of Alzheimer's disease-like pathology in 3xTg-AD mice. *Aging cell* 18: e12873

Bergles DE, Roberts JD, Somogyi P, Jahr CE. 2000. Glutamatergic synapses on oligodendrocyte precursor cells in the hippocampus. *Nature* 405: 187-91

Billings LM, Oddo S, Green KN, McGaugh JL, LaFerla FM. 2005. Intraneuronal Abeta causes the onset of early Alzheimer's disease-related cognitive deficits in transgenic mice. *Neuron* 45: 675-88

Boda E, Di Maria S, Rosa P, Taylor V, Abbracchio MP, Buffo A. 2014. Early phenotypic asymmetry of sister oligodendrocyte progenitor cells after mitosis and its modulation by aging and extrinsic factors. *Glia*

Brickman AM, Zahodne LB, Guzman VA, Narkhede A, Meier IB, et al. 2015. Reconsidering harbingers of dementia: progression of parietal lobe white matter hyperintensities predicts Alzheimer's disease incidence. *Neurobiol Aging* 36: 27-32

Butt AM, De La Rocha IC, Rivera A. 2019. Oligodendroglial Cells in Alzheimer's Disease. *Advances in experimental medicine and biology* 1175: 325-33

Butt AM, Hamilton N, Hubbard P, Pugh M, Ibrahim M. 2005. Synantocytes: the fifth element. *Journal of Anatomy* 207: 695-706

Chakroborty S, Hill ES, Christian DT, Helfrich R, Riley S, et al. 2019. Reduced presynaptic vesicle stores mediate cellular and network plasticity defects in an early-stage mouse model of Alzheimer's disease. *Molecular neurodegeneration* 14: 7-7

Chen TJ, Kula B, Nagy B, Barzan R, Gall A, et al. 2018. In Vivo Regulation of Oligodendrocyte Precursor Cell Proliferation and Differentiation by the AMPA-Receptor Subunit GluA2. *Cell reports* 25: 852-61.e7

Chvátal A, Anderová M, Hock M, Prajerová I, Neprasová H, et al. 2007. Three-dimensional confocal morphometry reveals structural changes in astrocyte morphology in situ. *J Neurosci Res* 85: 260-71

Clark JK, Furgerson M, Crystal JD, Fechheimer M, Furukawa R, Wagner JJ. 2015. Alterations in synaptic plasticity coincide with deficits in spatial working memory in presymptomatic 3xTg-AD mice. *Neurobiol Learn Mem* 125: 152-62

Crimins JL, Pooler A, Polydoro M, Luebke JI, Spires-Jones TL. 2013. The intersection of amyloid beta and tau in glutamatergic synaptic dysfunction and collapse in Alzheimer's disease. *Ageing research reviews* 12: 757-63

Dawson MR, Polito A, Levine JM, Reynolds R. 2003. NG2-expressing glial progenitor cells: an abundant and widespread population of cycling cells in the adult rat CNS. *Mol Cell Neurosci* 24: 476-88

De Rossi P, Buggia-Prevot V, Clayton BL, Vasquez JB, van Sanford C, et al. 2016. Predominant expression of Alzheimer's disease-associated BIN1 in mature oligodendrocytes and localization to white matter tracts. *Mol Neurodegener* 11: 59

Desai MK, Guercio BJ, Narrow WC, Bowers WJ. 2011. An Alzheimer's disease-relevant presenilin-1 mutation augments amyloid-beta-induced oligodendrocyte dysfunction. *Glia* 59: 627-40

Desai MK, Mastrangelo MA, Ryan DA, Sudol KL, Narrow WC, Bowers WJ. 2010. Early oligodendrocyte/myelin pathology in Alzheimer's disease mice constitutes a novel therapeutic target. *Am J Pathol* 177: 1422-35

Desai MK, Sudol KL, Janelsins MC, Mastrangelo MA, Frazer ME, Bowers WJ. 2009. Triple-transgenic Alzheimer's disease mice exhibit region-specific abnormalities in brain myelination patterns prior to appearance of amyloid and tau pathology. *Glia* 57: 54-65

Dimou L, Simon C, Kirchhoff F, Takebayashi H, Götz M. 2008. Progeny of Olig2-expressing progenitors in the gray and white matter of the adult mouse cerebral cortex. *The Journal of neuroscience : the official journal of the Society for Neuroscience* 28: 10434-42

Dong YX, Zhang HY, Li HY, Liu PH, Sui Y, Sun XH. 2018. Association between Alzheimer's disease pathogenesis and early demyelination and oligodendrocyte dysfunction. *Neural regeneration research* 13: 908-14

Fischer FU, Wolf D, Scheurich A, Fellgiebel A. 2015. Altered whole-brain white matter networks in preclinical Alzheimer's disease. *NeuroImage. Clinical* 8: 660-6

Horiuchi M, Maezawa I, Itoh A, Wakayama K, Jin LW, et al. 2012. Amyloid β1-42 oligomer inhibits myelin sheet formation in vitro. *Neurobiol Aging* 33: 499-509

Hoy AR, Ly M, Carlsson CM, Okonkwo OC, Zetterberg H, et al. 2017. Microstructural white matter alterations in preclinical Alzheimer's disease detected using free water elimination diffusion tensor imaging. *PLoS One* 12: e0173982

Hughes EG, Orthmann-Murphy JL, Langseth AJ, Bergles DE. 2018. Myelin remodeling through experience-dependent oligodendrogenesis in the adult somatosensory cortex. *Nat Neurosci* 21: 696-706

Ihara M, Polvikoski TM, Hall R, Slade JY, Perry RH, et al. 2010. Quantification of myelin loss in frontal lobe white matter in vascular dementia, Alzheimer's disease, and dementia with Lewy bodies. *Acta neuropathologica* 119: 579-89

Kang SH, Fukaya M, Yang JK, Rothstein JD, Bergles DE. 2010. NG2+ CNS glial progenitors remain committed to the oligodendrocyte lineage in postnatal life and following neurodegeneration. *Neuron* 68: 668-81

Kulijewicz-Nawrot M, Syková E, Chvátal A, Verkhratsky A, Rodríguez JJ. 2013. Astrocytes and glutamate homoeostasis in Alzheimer's disease: a decrease in glutamine synthetase, but not in glutamate transporter-1, in the prefrontal cortex. *ASN Neuro* 5: 273-82

Levine J. 2016. The reactions and role of NG2 glia in spinal cord injury. *Brain Res* 1638: 199-208

Li W, Tang Y, Fan Z, Meng Y, Yang G, et al. 2013. Autophagy is involved in oligodendroglial precursor-mediated clearance of amyloid peptide. *Mol Neurodegener* 8: 27

Mastrangelo MA, Bowers WJ. 2008. Detailed immunohistochemical characterization of temporal and spatial progression of Alzheimer's disease-related pathologies in male triple-transgenic mice. *BMC Neurosci* 9: 81

McKenzie AT, Moyon S, Wang M, Katsyv I, Song WM, et al. 2017. Multiscale network modeling of oligodendrocytes reveals molecular components of myelin dysregulation in Alzheimer's disease. *Mol Neurodegener* 12: 82

McKenzie IA, Ohayon D, Li H, de Faria JP, Emery B, et al. 2014. Motor skill learning requires active central myelination. *Science* 346: 318-22

Mitew S, Kirkcaldie MT, Halliday GM, Shepherd CE, Vickers JC, Dickson TC. 2010. Focal demyelination in Alzheimer's disease and transgenic mouse models. *Acta neuropathologica* 119: 567-77

Nasrabady SE, Rizvi B, Goldman JE, Brickman AM. 2018. White matter changes in Alzheimer's disease: a focus on myelin and oligodendrocytes. *Acta neuropathologica communications* 6: 22-22

Ndayisaba A, Kaindlstorfer C, Wenning GK. 2019. Iron in Neurodegeneration - Cause or Consequence? *Frontiers in neuroscience* 13: 180

Neumann B, Baror R, Zhao C, Segel M, Dietmann S, et al. 2019. Metformin Restores CNS Remyelination Capacity by Rejuvenating Aged Stem Cells. *Cell Stem Cell* 25: 473-85.e8

Nie X, Falangola MF, Ward R, McKinnon ET, Helpern JA, et al. 2019. Diffusion MRI detects longitudinal white matter changes in the 3xTg-AD mouse model of Alzheimer's disease. *Magn Reson Imaging* 57: 235-42

Nielsen HM, Ek D, Avdic U, Orbjörn C, Hansson O, et al. 2013. NG2 cells, a new trail for Alzheimer's disease mechanisms? *Acta Neuropathol Commun* 1: 7

Nielsen HM, Mulder SD, Beliën JA, Musters RJ, Eikelenboom P, Veerhuis R. 2010. Astrocytic A beta 1-42 uptake is determined by A beta-aggregation state and the presence of amyloid-associated proteins. *Glia* 58: 1235-46

Oddo S, Caccamo A, Shepherd JD, Murphy MP, Golde TE, et al. 2003. Triple-transgenic model of Alzheimer's disease with plaques and tangles: intracellular Abeta and synaptic dysfunction. *Neuron* 39: 409-21

Olabarria M, Noristani HN, Verkhratsky A, Rodríguez JJ. 2010. Concomitant astroglial atrophy and astrogliosis in a triple transgenic animal model of Alzheimer's disease. *Glia* 58: 831-8

Ong WY, Levine JM. 1999. A light and electron microscopic study of NG2 chondroitin sulfate proteoglycan-positive oligodendrocyte precursor cells in the normal and kainate-lesioned rat hippocampus. *Neuroscience* 92: 83-95

Psachoulia K, Jamen F, Young KM, Richardson WD. 2009. Cell cycle dynamics of NG2 cells in the postnatal and ageing brain. *Neuron Glia Biol* 5: 57-67

Rivera A, Vanzuli I, Arellano JJ, Butt A. 2016. Decreased Regenerative Capacity of Oligodendrocyte Progenitor Cells (NG2-Glia) in the Ageing Brain: A Vicious Cycle of Synaptic Dysfunction, Myelin Loss and Neuronal Disruption? *Current Alzheimer research* 13: 413-8

Rivers LE, Young KM, Rizzi M, Jamen F, Psachoulia K, et al. 2008. PDGFRA/NG2 glia generate myelinating oligodendrocytes and piriform projection neurons in adult mice. *Nat Neurosci* 11: 1392-401

Rodríguez JJ, Butt AM, Gardenal E, Parpura V, Verkhratsky A. 2016. Complex and differential glial responses in Alzheimer's disease and ageing. *Current Alzheimer research* 13: 343-58

Rodríguez JJ, Jones VC, Tabuchi M, Allan SM, Knight EM, et al. 2008. Impaired adult neurogenesis in the dentate gyrus of a triple transgenic mouse model of Alzheimer's disease. *PLoS One* 3: e2935

Rodríguez JJ, Terzieva S, Olabarria M, Lanza RG, Verkhratsky A. 2013. Enriched environment and physical activity reverse astrogliodegeneration in the hippocampus of AD transgenic mice. *Cell Death Dis* 4: e678

Roher AE, Weiss N, Kokjohn TA, Kuo YM, Kalback W, et al. 2002. Increased A beta peptides and reduced cholesterol and myelin proteins characterize white matter degeneration in Alzheimer's disease. *Biochemistry* 41: 11080-90

Segel M, Neumann B, Hill MFE, Weber IP, Viscomi C, et al. 2019. Niche stiffness underlies the ageing of central nervous system progenitor cells. *Nature* 573: 130-34

Sim FJ, Zhao C, Penderis J, Franklin RJ. 2002. The age-related decrease in CNS remyelination efficiency is attributable to an impairment of both oligodendrocyte progenitor recruitment and differentiation. *The Journal of neuroscience : the official journal of the Society for Neuroscience* 22: 2451-9

Stallcup WB. 1981. The NG2 antigen, a putative lineage marker: immunofluorescent localization in primary cultures of rat brain. *Developmental biology* 83: 154-65

Stassart RM, Mobius W, Nave KA, Edgar JM. 2018. The Axon-Myelin Unit in Development and Degenerative Disease. *Frontiers in neuroscience* 12: 467

Wake H, Lee PR, Fields RD. 2011. Control of local protein synthesis and initial events in myelination by action potentials. *Science* 333: 1647-51

Wang F, Ren SY, Chen JF, Liu K, Li RX, et al. 2020. Myelin degeneration and diminished myelin renewal contribute to age-related deficits in memory. *Nat Neurosci*

Wang R, Reddy PH. 2017. Role of Glutamate and NMDA Receptors in Alzheimer's Disease. *Journal of Alzheimer's disease : JAD* 57: 1041-48

Xiao L, Ohayon D, McKenzie IA, Sinclair-Wilson A, Wright JL, et al. 2016. Rapid production of new oligodendrocytes is required in the earliest stages of motor-skill learning. *Nat Neurosci* 19: 1210-7

Yin F, Sancheti H, Patil I, Cadenas E. 2016. Energy metabolism and inflammation in brain aging and Alzheimer's disease. *Free radical biology & medicine* 100: 108-22

Young KM, Psachoulia K, Tripathi RB, Dunn S-J, Cossell L, et al. 2013. Oligodendrocyte dynamics in the healthy adult CNS: evidence for myelin remodeling. *Neuron* 77: 873-85

Zhan X, Jickling GC, Ander BP, Stamova B, Liu D, et al. 2015. Myelin basic protein associates with AbetaPP, Abeta1-42, and amyloid plaques in cortex of Alzheimer's disease brain. *Journal of Alzheimer's disease : JAD* 44: 1213-29

Zhang P, Kishimoto Y, Grammatikakis I, Gottimukkala K, Cutler RG, et al. 2019a. Senolytic therapy alleviates Abeta-associated oligodendrocyte progenitor cell senescence and cognitive deficits in an Alzheimer's disease model. *Nat Neurosci* 22: 719-28

Zhang P, Kishimoto Y, Grammatikakis I, Gottimukkala K, Cutler RG, et al. 2019b. Senolytic therapy alleviates Aβ-associated oligodendrocyte progenitor cell senescence and cognitive deficits in an Alzheimer's disease model. *Nat Neurosci* 22: 719-28

Zhu X, Hill RA, Dietrich D, Komitova M, Suzuki R, Nishiyama A. 2011. Age-dependent fate and lineage restriction of single NG2 cells. *Development* 138: 745-53

Zhu X, Hill RA, Nishiyama A. 2008. NG2 cells generate oligodendrocytes and gray matter astrocytes in the spinal cord. *Neuron Glia Biol* 4: 19-26

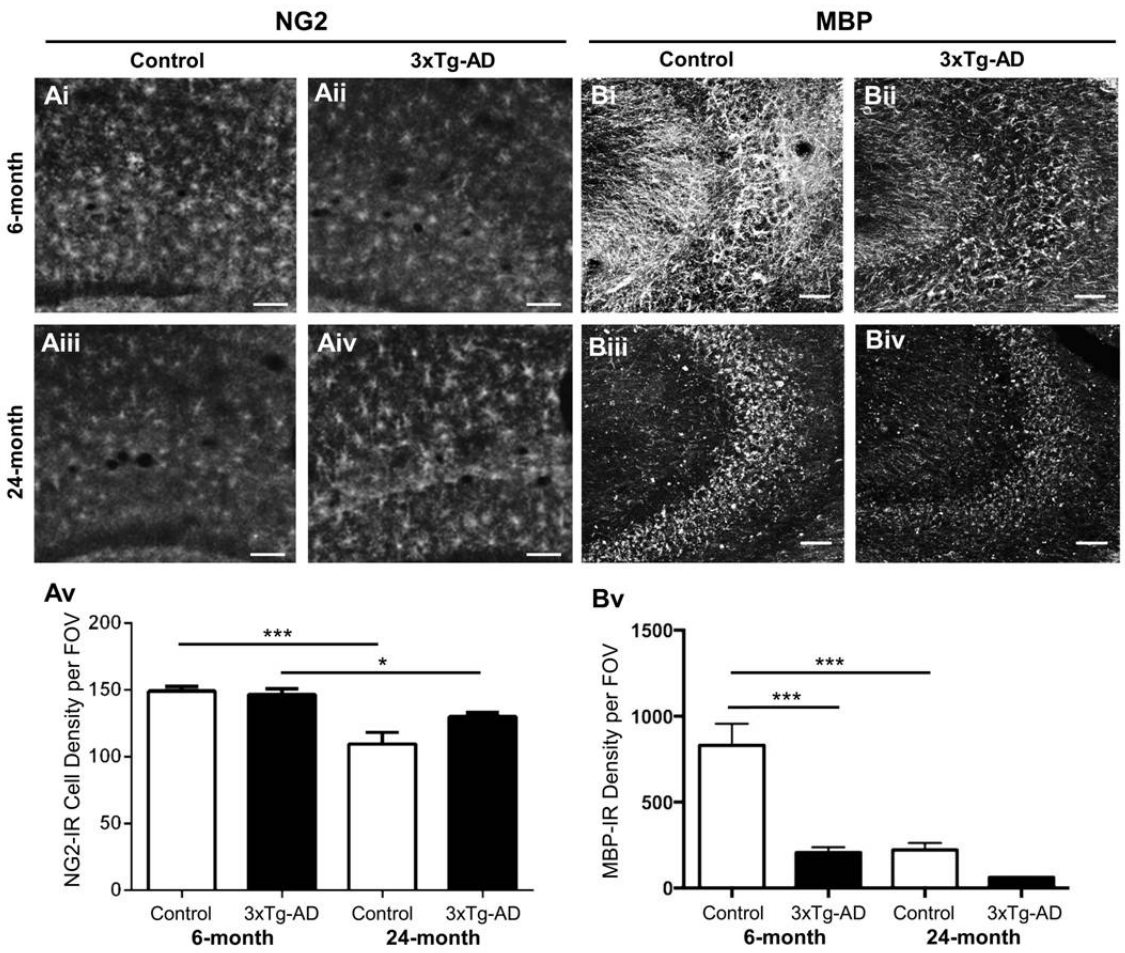
NG2
MBP
Control
3xTg-AD
Control
3xTg-AD
6-month
24-month
Ai
Aii
Bi
Bii
Aiii
Aiv
Biii
Biv
Av
NG2-IR Cell Density per FOV
200
150
100
50
0
***
*
Control
3xTg-AD
Control
3xTg-AD
6-month
24-month
Bv
MBP-IR Density per FOV
1500
1000
500
0
***
***
Control
3xTg-AD
Control
3xTg-AD
6-month
24-month

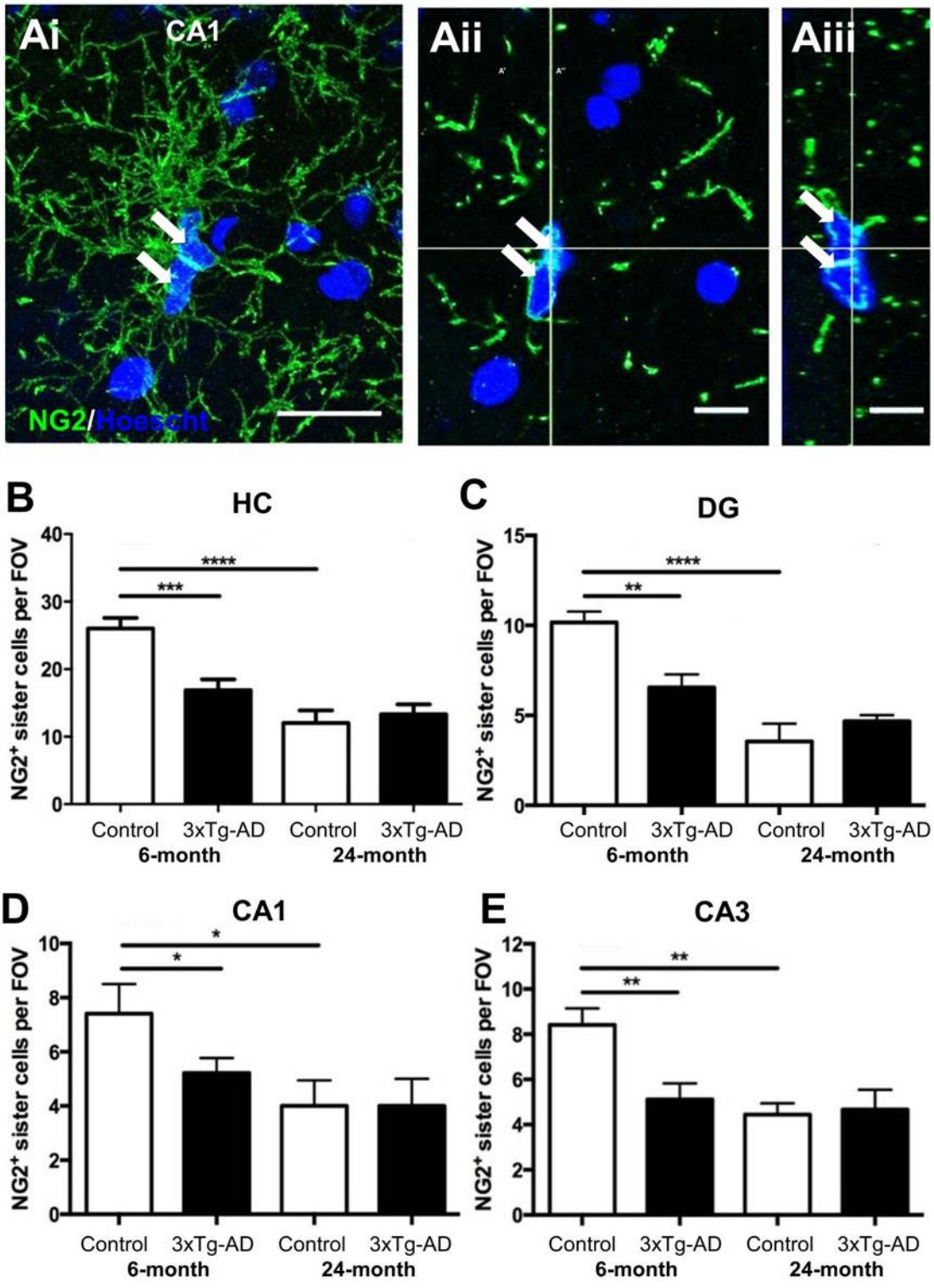
Ai
CA1
NG2/Hoescht
Aii
Aiii
B
HC
NG2+ sister cells per FOV
40
30
20
10
0
****
***
Control
3xTg-AD
Control
3xTg-AD
6-month
24-month
C
DG
NG2+ sister cells per FOV
15
10
5
0
****
**
Control
3xTg-AD
Control
3xTg-AD
6-month
24-month
D
CA1
NG2+ sister cells per FOV
10
8
6
4
2
0
*
*
Control
3xTg-AD
Control
3xTg-AD
6-month
24-month
E
CA3
NG2+ sister cells per FOV
12
10
8
6
4
2
0
**
**
Control
3xTg-AD
Control
3xTg-AD
6-month
24-month

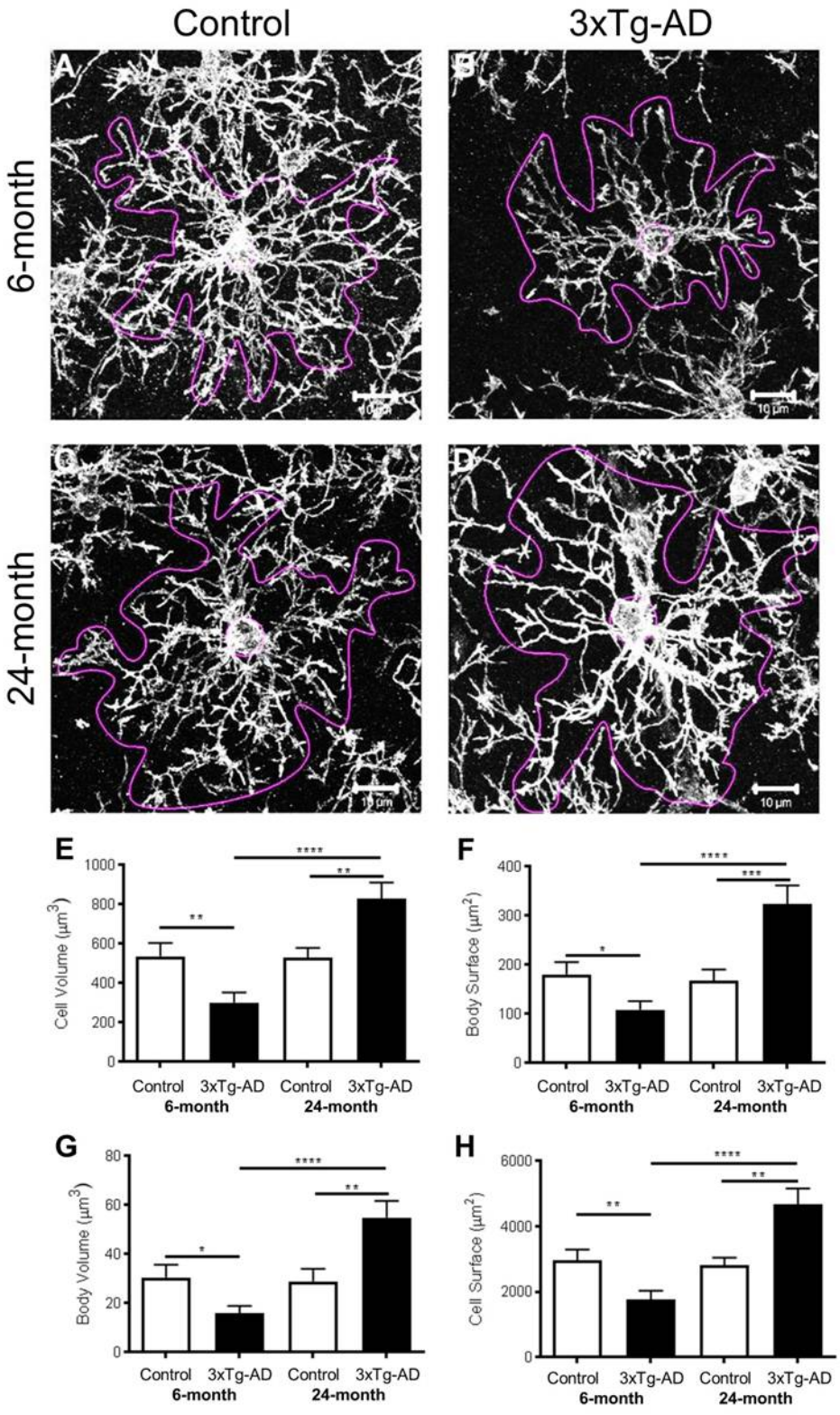
Control
3xTg-AD
6-month
24-month
A
B
C
D
10 µm
E
Cell Volume (µm3)
F
Body Surface (µm2)
G
Body Volume (µm3)
H
Cell Surface (µm2)
Control
3xTg-AD
6-month
24-month

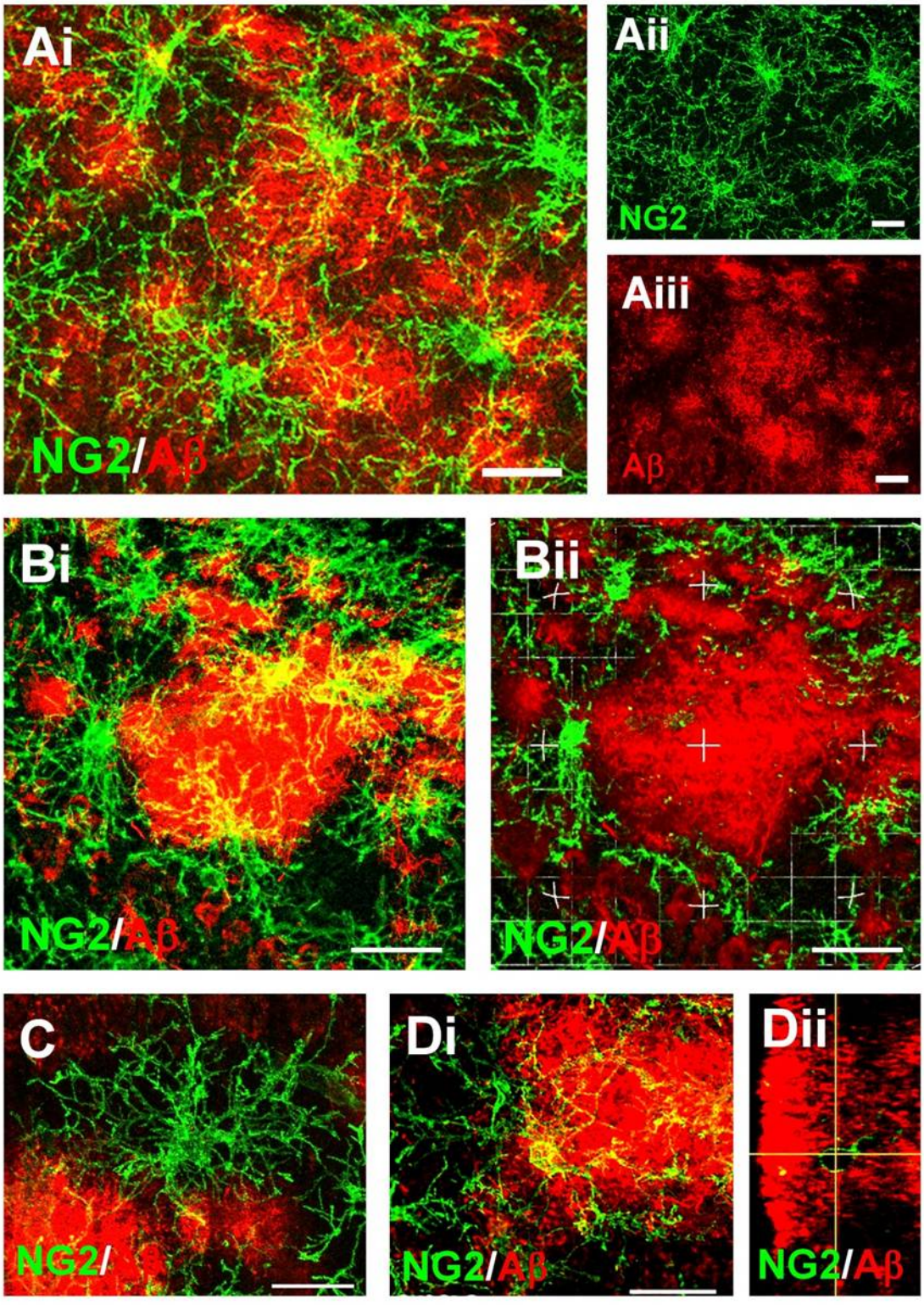
Ai
NG2/Aβ
Aii
NG2
Aiii
Aβ
Bi
NG2/Aβ
Bii
NG2/Aβ
C
NG2/
Di
NG2/Aβ
Dii
NG2/Aβ

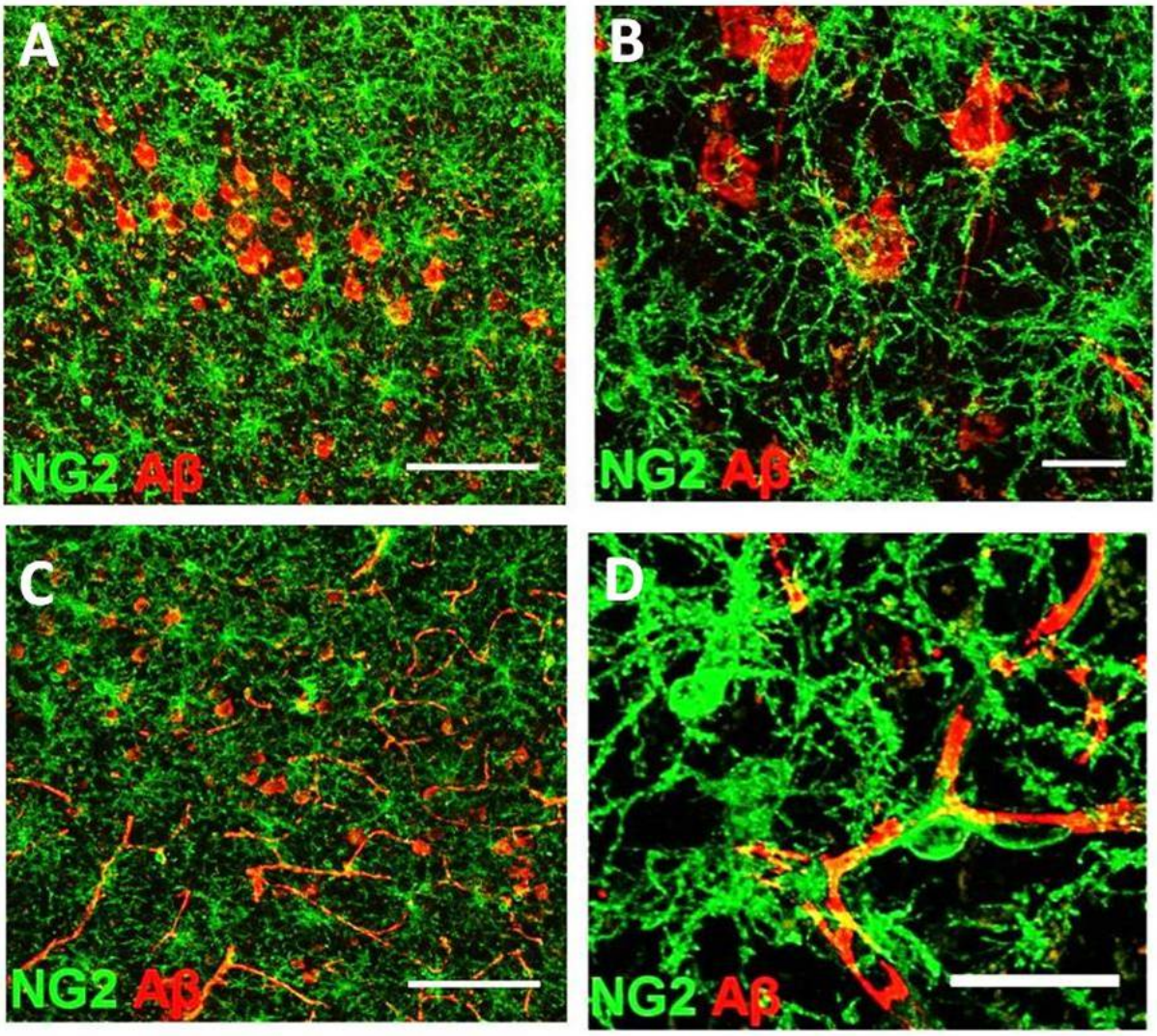
A
NG2 Aβ
B
NG2 Aβ
C
NG2 Aβ
D
NG2 Aβ

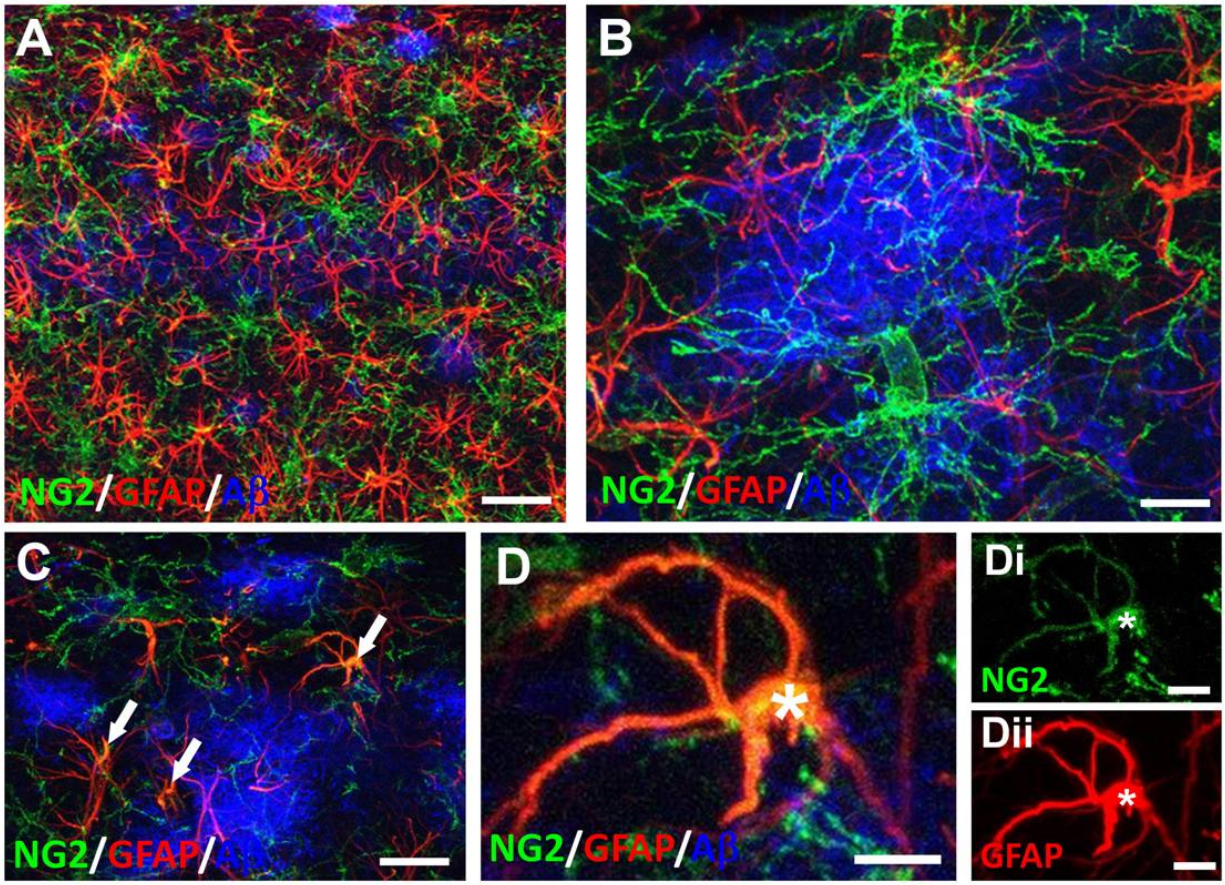
A
NG2/GFAP/Aβ
B
NG2/GFAP/Aβ
C
NG2/GFAP/Aβ
D
NG2/GFAP/Aβ
Di
NG2
Dii
GFAP

Highlights

- Life-long generation of myelin is the function of adult oligodendrocyte progenitor cells (OPCs)
- Age-related loss of myelin is accelerated in the 3xTg-AD mouse model of Alzheimer's disease (AD).
- OPCs are disrupted at an early stage of 3xTg-AD
- Dysregulation of OPC and myelin loss are important biomarkers for AD-like pathology

Verification:

1. All authors have disclose actual or potential conflicts of interest. Arthur Butt and Andrea Rivera are share owners in the company GliaGenesis. The other authors have no actual or potential conflicts of interest.

We verify that none of the authors' institution' have contracts relating to this research through which it or any other organization may stand to gain financially now or in the future.

We verify there are no agreements of authors or their institutions that could be seen as involving a financial interest in this work.

2. The work described was funded from multiple grants, which are fully disclosed. We verify authors have disclosed all sources of financial support related to the manuscript being submitted.

3. We verify that the data contained in the manuscript being submitted have not been previously published, have not been submitted elsewhere and will not be submitted elsewhere while under consideration at Neurobiology of Aging.

4. We verify a statement is included that all animal procedures were carried out in accordance with the United Kingdom Animals (Scientific Procedures) Act of 1986 under licence from the Home Office.

5. We verify that all authors have reviewed the contents of the manuscript being submitted, approve of its contents and validate the accuracy of the data.

Credit Author Statement

We encourage you to submit an author statement file outlining all authors' individual contributions, using the relevant CRediT roles: Conceptualization; Data curation; Formal analysis; Funding acquisition; Investigation; Methodology; Project administration; Resources; Software; Supervision; Validation; Visualization; Roles/Writing - original draft; Writing - review & editing. Please format with author name first followed by the CRediT roles: for an example and more details see authorship of a paper section

Ilaria Vanzulli: Formal Analysis; Investigation; Methodology; Writing - original draft.
Maria Papanikolaou: Formal Analysis; Investigation; Methodology; Validation.
Irene Chacon De La Rocha: Investigation; Methodology; Validation.
Francesca Pieropan: Investigation; Methodology; Validation.
Andrea D. Rivera: Investigation.
Diego Gomez-Nicola: Writing - review & editing.
Alexei Verkhratsky: Conceptualization; Writing - review & editing.
José Julio Rodríguez: Conceptualization; Resources; Software; Writing - review & editing
Arthur M. Butt: Conceptualization; Data curation; Formal analysis; Funding acquisition; Project administration; Resources; Supervision; Validation; Visualization; Writing - original draft; Writing - review & editing.